*PROC. BULK POWER SYSTEM VOLTAGE PHENOMENA–III SEMINAR*, DAVOS, SWITZERLAND, AUGUST 1994, PP. 349–358.

# IMPROVING CONTINUATION METHODS FOR TRACING BIFURCATION DIAGRAMS IN POWER SYSTEMS

**Claudio A. Cañizares** **Antonio Z. de Souza** **Victor H. Quintana**
University of Waterloo
Department of Electrical & Computer Engineering
Waterloo, ON, Canada N2L 3G1

**Abstract**: This paper proposes several techniques for reducing the computational burden of tracing bifurcation diagrams in power systems with continuation methods. The first technique described in the paper is an implementation of the fast-decoupled method in the predictor-corrector continuation algorithm. The other proposed techniques consist on reducing the system size. One reduction method is based on the tangent vector calculated during the predictor step, whereas the second one is based on network partition and detection of voltage-weak areas. The computational issues related to the actual implementation of these methods are also discussed. The system reduction techniques are tested in the 300 bus IEEE system, so that these methods can be analyzed in a realistic environment.

**Keywords**: continuation methods, generic saddle-node bifurcations, system reduction, fast-decoupled methods.

## 1. Introduction

Voltage stability problems in power systems arise from a variety of reasons and operating conditions, from voltage control problems (taps, automatic voltage regulators, HVDC controls [2]–[6]) to system bifurcations (saddle-nodes, transcriticals, Hopfs [2, 6]–[18]). Local bifurcations are characterized by one or two system eigenvalues lying on the imaginary axis of the complex plane for certain system parameters values, i.e., a real eigenvalue (saddle-node, transcritical, pitchfork bifurcations) or the real part of a complex conjugate pair (Hopf bifurcation) become zero for given values of these parameters. Thus, the power system moves from one stable equilibrium point (s.e.p.) to another as the parameters (load and generation powers, taps, control settings, etc.) change slowly, until certain parameters values are reached and the system "bifurcates," i.e., the eigenvalues reach the imaginary axis. This phenomenon can be classified as a steady-state stability problem [2]; however the final result is a system-wide dynamic instability [7]–[10].

Bifurcations of one-parameter dynamic systems have been thoroughly studied in differential equation models [19, 20]. Several authors have extended this theory to the analysis of similar phenomena in power system models [8, 9, 10, 11, 15, 16, 17, 18], which are typically represented by a set of differential equations and algebraic constraints. Particularly, in [16, 17] the author thoroughly discusses the conditions and methods used for detecting saddle-node bifurcations in these kinds of models.

Of all local bifurcations, only saddle-nodes and Hopfs are generic, i.e., one expects to encounter these types of bifurcations unless there are some special assumptions regarding the system modeling [19, 20]; this can be demonstrated in power system models for certain system parameters [18]. Therefore, this paper also concentrates on these two kinds of bifurcations in power networks.

Bifurcations points can be located using direct and/or continuation methods [20]. Direct methods are designed to find the bifurcation from a known operating condition in one solution attempt, whereas continuation methods trace a succession the equilibrium points by automatically changing the parameter value until the bifurcation is encountered, and beyond. The manifold resulting from joining the system equilibria generated by the continuation method is known as the bifurcation diagram ("PV", "QV", or "nose" curves are particular cases of these diagrams). For power systems models, direct and continuation methods have been proven to be numerically well-behaved [16, 17]. Direct methods have been shown to be an efficient way of locating saddle-nodes when a system is close to these bifurcations points [6]; however, when the system is far from bifurcation, and especially when all system control and limits are considered, this method tends to fail [6]. Locating Hopf bifurcations with these methods is completely impractical as demonstrated in [18]. On the other hand, continuation methods do not present these difficulties and have the additional advantage of yielding more information than direct methods, since complete bifurcation diagrams for any type of bifurcation can be generated with this technique; however, this method is time consuming, particularly when dealing with large networks [6].

This paper concentrates on discussing several issues associated to the detection of generic saddle-node bifurcations with the continuation method. Locating Hopf bifurcations does not represent a particularly difficult numerical problem when continuation methods are used, since these bifurcations do not produce a singularity of the system equations Jacobian or a change in the number of system equilibrium points; one can detect these bifurcations by monitoring the eigenvalues of system equilibria on the bifurcation diagram using typical eigenvalue computational techniques.

Several authors have proposed different implementations of the continuation method to detect saddle-node bifurcations in power systems [6, 21]–[26]. These programs can also be used to detect other types of bifurcations as shown in [18], since they are slight variations, based on some typical characteristics of power system models, of the techniques described in [20]. In [22], a tangent vector predictor together with a perpendicular intersection corrector are used to trace part of the bifurcation diagram, whereas in [23, 25] a parameterization technique with a fixed parameter corrector are proposed to avoid singularities of the continuation method Jacobians at saddle-node bifurcation points, so that complete bifurcation diagrams can be traced. The authors in [6, 21] use similar predictor and corrector techniques as in [22], but introduce a step length control technique to avoid the need of parameter-

ization when tracing whole bifurcation diagrams, and to efficiently handle system limits and control mode changes, particularly when high voltage direct current (HVDC) systems are included. In [24] an optimal step length control is proposed to deal effectively with Q-limits in generators. Finally, the authors in [26] propose the use of a secant predictor and an arc-length parameterization. Section 2 discusses with detail all of these techniques, concentrating on the advantages and disadvantages of each one of them.

The problem of large CPU times required by the continuation method when tracing bifurcation diagrams was discussed in [6]; little has been reported in the literature, however, on trying to overcome this difficulty. This paper addresses this issue by proposing different techniques to reduce CPU time, so that continuation methods can be efficiently used in a control center environment for "real time" applications. Two distinct techniques are proposed and studied, namely fast-decoupled methods and system reductions. The introduction of fast-decoupled methods into the continuation method is analyzed in detail in section 3, concentrating on the computational issues related to the implementation of these techniques in existing programs. In section 4, two different methods to reduce the number of system buses to trace bifurcation diagrams are proposed and discussed. The system reduction techniques are finally tested in the 300 bus IEEE system, so that several computational issues can be addressed in a realistic environment.

## 2. Continuation Method

A power system can be modeled using a set of nonlinear ordinary differential equations and algebraic constraints, such as

$$\begin{aligned} \dot{\mathbf{x}} &= \mathbf{f}(\mathbf{x}, \mathbf{y}, \lambda) \\ \mathbf{0} &= \mathbf{g}(\mathbf{x}, \mathbf{y}, \lambda) \end{aligned} \tag{1}$$

where the vector $\mathbf{x} \in \Re^n$ represents the system state variables, the vector $\mathbf{y} \in \Re^m$ corresponds to the system variables associated to the nonlinear algebraic constraints, and $\lambda \in \Re^+$ is a slow changing parameter that drives the reduced system

$$\dot{\mathbf{x}} = \mathbf{s}(\mathbf{x}, \lambda) = \mathbf{f}(\mathbf{x}, \mathbf{h}(\mathbf{x}), \lambda) \tag{2}$$

to a local generic saddle-node or Hopf bifurcation, if along system trajectories of interest one has a nonsingular Jacobian of the algebraic constraints $D_y\mathbf{g}(\cdot)$. Furthermore, as demonstrated in [16, 17] for this particular assumption, a saddle-node bifurcation point of (2) corresponds to a system equilibrium point where the Jacobian $D_z\mathbf{F}(\mathbf{z}_0, \lambda_0)$ is singular ($\mathbf{F}(\cdot) \triangleq [\mathbf{f}^T(\cdot)\ \mathbf{g}^T(\cdot)]^T$, $\mathbf{z} \triangleq [\mathbf{x}^T\ \mathbf{y}^T]^T$, $\mathbf{F}(\mathbf{z}_0, \lambda_0) = \mathbf{0}$). Thus, a bifurcation manifold of differential equations (2) can be traced by monitoring the equilibria of (1).

Voltage profiles of power systems have been typically obtained by calculating a series of equilibrium points of equations (1) with successive power flow solutions [2, 27]. These profiles correspond to parts of the bifurcation diagram. Hence, by solving $\mathbf{F}(\mathbf{z}, \lambda) = \mathbf{0}$ for increasing values of $\lambda$, one can easily trace relevant parts of the bifurcation diagram; however, since the system Jacobian becomes singular at a saddle-node bifurcation $(\mathbf{z}_0, \lambda_0)$, and no equilibrium points or solutions exist for values of $\lambda > \lambda_0$, one cannot accurately compute $\lambda_0$ using this simple technique, because divergence of the Newton-Raphson based numerical methods does not guarantee nonexistence of solutions of the corresponding equations. Nevertheless, as shown in [2, 10], this method can be used to obtain solutions rather close to the saddle-node bifurcation point due to the highly nonlinear behavior of the eigenvalues of the system Jacobian. Figure 1 depicts the minimum magnitudes of the eigenvalues and singular values of the steady-state Jacobian for a simple power system constituted of a generator, a transmission line, and a constant power factor PQ load, where the active load power $P$ is chosen as the slow varying parameter that drives the system to bifurcation. Notice the sharp change in the magnitude of the eigenvalues and singular values when the system is close to the bifurcation point. Similar behavior has been also observed by several researchers in a variety of power systems [7, 13, 28]. The Voltage Stability Analysis (VSTAB) program distributed by the Electric Power Research Institute (EPRI), uses this technique to successfully trace the stable equilibrium region of the bifurcation diagram for a variety of power system models [27].

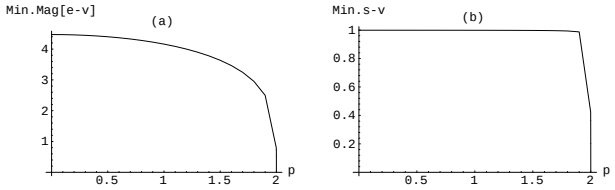


**Fig. 1:** *(a) Minimum magnitude of the eigenvalues and (b) singular values of the s.e.p.s of a simple generator-line-load power system, as a function of the system load P.*

The continuation method overcomes the difficulties of the successive power flow solutions method, allowing the user to trace the complete bifurcation diagram by automatically changing the value of $\lambda$. The strategy used in this method is illustrated in Fig. 2, where a known equilibrium point $(\mathbf{z}_1, \lambda_1)$ of the bifurcation manifold is used to compute the direction vector $\Delta\mathbf{z}_1$ and a change $\Delta\lambda_1$ of the system parameter. This first step is known as the predictor, since it generates an initial guess $(\mathbf{z}_1 + \Delta\mathbf{z}_1, \lambda_1 + \Delta\lambda_1)$, which is then used in the corrector step to compute a new equilibrium point $(\mathbf{z}_2, \lambda_2)$ on the bifurcation diagram. Since the Jacobian $D_z\mathbf{F}|_0$ is singular at the bifurcation point, a parameterization is sometimes needed in the predictor and/or corrector steps, depending on the techniques used, to guarantee a well behaved numerical solution of the related equations. A detailed description of these techniques follows.

### 2.1. Predictor and Parameterization

One way of calculating the direction vector $\Delta\mathbf{z}_1$ at an equilibrium point $(\mathbf{z}_1, \lambda_1)$ on the bifurcation manifold, is to compute the tangent vector to the manifold at that point. Hence, since $\mathbf{F}(\mathbf{z}_1, \lambda_1) = \mathbf{0}$, then

$$\begin{aligned} &\frac{\mathrm{d}\mathbf{F}}{\mathrm{d}\lambda}(\mathbf{z}_1, \lambda_1) = D_z\mathbf{F}(\mathbf{z}_1, \lambda_1)\ \left.\frac{\mathrm{d}\mathbf{z}}{\mathrm{d}\lambda}\right|_1 + \left.\frac{\partial\mathbf{F}}{\partial\lambda}\right|_1 = \mathbf{0} \\ \Rightarrow\quad & D_z\mathbf{F}|_1\ \left.\frac{\mathrm{d}\mathbf{z}}{\mathrm{d}\lambda}\right|_1 = -\left.\frac{\partial\mathbf{F}}{\partial\lambda}\right|_1 \end{aligned} \tag{3}$$

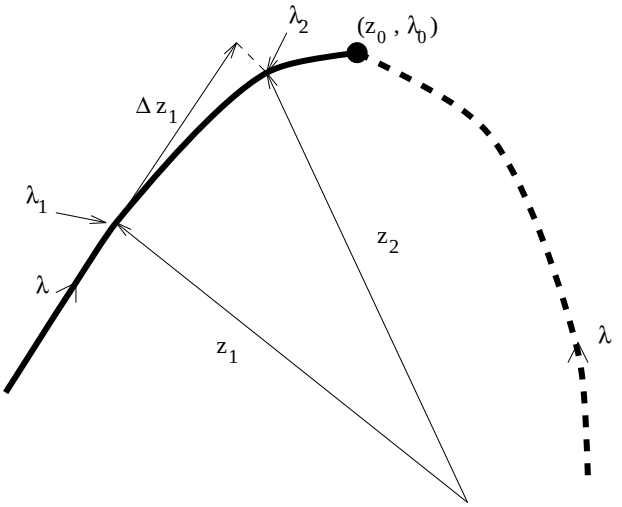


**Fig. 2:** *Bifurcation diagram in state and parameter space depicting the s.e.p.s with a continuos bold line, the u.e.p.s with a bold dashed line, and the bifurcation point at* $(\mathbf{z}_0, \lambda_0)$*. A continuation methodology to move from one equilibrium point* $(\mathbf{z}_1, \lambda_1)$ *to another* $(\mathbf{z}_2, \lambda_2)$ *is also shown.*

Thus, the direction vector and the parameter step come from the normalization of the tangent vector, i.e.,

$$\begin{aligned} \Delta\lambda_1 &= \frac{k}{\| \, \mathrm{d}\mathbf{z}/\mathrm{d}\lambda|_1 \, \|} \\ \Delta\mathbf{z}_1 &= \Delta\lambda_1 \left.\frac{\mathrm{d}\mathbf{z}}{\mathrm{d}\lambda}\right|_1 \end{aligned} \tag{4}$$

where $k \in \Re^+$ is a constant that controls the size of the predictor step. The normalization in (4) results on the reduction of the step size as the system approaches the saddle-node bifurcation point, since the magnitude of the tangent vector increases as the system gets closer to this point. If the step is too large, then the initial guess $(\mathbf{z}_1 + \Delta\mathbf{z}_1, \lambda_1 + \Delta\lambda_1)$ yield convergence problems in the corrector, whereas if the step is too small, the method takes too many steps to trace the bifurcation manifold. A technique to determine the optimal value of $k$ was proposed in [24], considering the reactive power limits of the generators. Good results were reported in [6] for $k = 1$ in various system sizes, by using step cutting when limits or convergence problems are encountered.

This predictor technique has the particular advantage of generating an approximation to the zero right-eigenvector at the bifurcation point, since the tangent vector smoothly converges to this eigenvector [16, 17]. The zero right-eigenvector yields important information regarding voltage sensitive areas in the system [12, 29]

Computing the tangent vector in (3) does not represent a significant computational cost, since one can use the last factored Jacobian matrix $D_z\mathbf{F}(\mathbf{z}_1, \lambda_1)$. However, this method has difficulties when the equilibrium point is close to the bifurcation point, since the system Jacobian becomes ill-conditioned. To avoid this problem parameterization techniques can be used [20]. A relatively simple technique successfully applied in [6, 21, 23, 24] is local parameterization, which consists on interchanging close to the bifurcation the parameter $\lambda$ with the system variable $z_i \in \mathbf{z}$ that has the largest normalized entry in the tangent vector, so that $\lambda$ becomes part of the equations variables, whereas $z_i$ becomes the new parameter $p$, i.e., for $N \triangleq n + m$

$$p \leftarrow \max\left\{ \left|\frac{\Delta z_1}{z_1}\right|, \left|\frac{\Delta z_2}{z_2}\right|, \ldots, \left|\frac{\Delta z_N}{z_N}\right|, \left|\frac{\Delta\lambda}{\lambda}\right| \right\} \tag{5}$$

Nevertheless, when step cutting and perpendicular intersection correctors are used, this local parameterization is not needed in practice [6, 21], due to the highly nonlinear behavior of the Jacobian eigenvalues; one must be rather close to the saddle-node bifurcation point in order to have an ill-conditioned Jacobian matrix.

Another type of predictor with parameterization used to take the system around the singularity of the bifurcation point is the arclength method [20, 26]. This technique is based on the idea that the system variables and parameter at the equilibrium points can be represented as a function of the arclength $s$ of the bifurcation manifold, i.e., for $\mathbf{F}(\mathbf{z}_1(s), \lambda_1(s)) = \mathbf{0}$,

$$D_z\mathbf{F}|_1 \left.\frac{\mathrm{d}\mathbf{z}}{\mathrm{d}s}\right|_1 + \left.\frac{\partial\mathbf{F}}{\partial\lambda}\right|_1 \left.\frac{\mathrm{d}\lambda}{\mathrm{d}s}\right|_1 = \mathbf{0} \tag{6}$$

where the arclength $s$ must satisfy the condition

$$\left.\frac{\mathrm{d}\mathbf{z}}{\mathrm{d}s}\right|_1^T \left.\frac{\mathrm{d}\mathbf{z}}{\mathrm{d}s}\right|_1 + \left.\frac{\mathrm{d}\lambda}{\mathrm{d}s}\right|_1^2 = 1 \tag{7}$$

Therefore, by approximating $\Delta\mathbf{z} \approx \mathrm{d}\mathbf{z}$, $\Delta\lambda \approx \mathrm{d}\lambda$, and $k = \Delta s \approx \mathrm{d}s$ $(k \in \Re^+)$, equations (6) and (7) become

$$\begin{aligned} D_z\mathbf{F}|_1\Delta\mathbf{z}_1 + \left.\frac{\partial\mathbf{F}}{\partial\lambda}\right|_1 \Delta\lambda_1 &= \mathbf{0} \\ \Delta\mathbf{z}_1^T\Delta\mathbf{z}_1 + \Delta\lambda_1^2 &= k \end{aligned} \tag{8}$$

where $k$ is a scalar constant that defines the length of the arc, and consequently the size of the predictor step. Equations (8) can be used to calculate the predictor step instead of equations (3) and (4), with a guaranteed nonsingular Jacobian at the bifurcation point.

Finally, a simpler predictor method that does not require of parameterization is the secant method, which was used in power systems bifurcation analysis in [26]. This technique consists on approximating the tangent vector $\mathrm{d}\mathbf{z}/\mathrm{d}\lambda$ using two or more previously determined equilibria on the bifurcation manifold. Thus, given two equilibrium points $(\mathbf{z}_1^a, \lambda_1^a)$ and $(\mathbf{z}_1^b, \lambda_1^b)$ on the bifurcation diagram, such that $\lambda_1^b > \lambda_1^a$,

$$\left.\frac{\mathrm{d}\mathbf{z}}{\mathrm{d}\lambda}\right|_1 \approx \mathbf{z}_1^b - \mathbf{z}_1^a$$

Equations (4) can then be used to calculate the direction vector and the parameter step. Notice that the closer these two points are, within reasonable numerical tolerances, the better the approximation of the tangent vector; however, more equilibrium points have to be computed, taking longer to trace the desired bifurcation diagram. On the other hand, points too far apart generate inadequate approximations of $\mathrm{d}\mathbf{z}/\mathrm{d}\lambda$, yielding initial guesses that lead to convergence difficulties during the corrector step. Using more points on the bifurcation manifold to better predict its curvature, requires of greater computational resources, but can be used as an alternative procedure to approximate the tangent vector when the bifurcation diagram changes direction rapidly, particularly when

control limits are encountered. Hence, depending on the curvature of the bifurcation diagram, the secant method presents advantages and disadvantages with respect to the two predictors previously described. A mixed approach is proposed in [20, 26], using the secant predictor when the tangent vector changes slowly on the "flat" part of the bifurcation diagram, to then switch to tangent vector or arclength predictors when the manifold presents larger curvatures.

### *2.2. Corrector*

Once an initial guess $(\mathbf{z}_1 + \Delta\mathbf{z}_1, \lambda_1 + \Delta\lambda_1)$ is determined in the predictor step, with or without parameterization, the actual equilibrium point $(\mathbf{z}_2, \lambda_2)$ on the bifurcation manifold must be calculated by solving the following set of equations for $\mathbf{z}$ and $\lambda$ [20]:

$$\begin{aligned} \mathbf{F}(\mathbf{z}, \lambda) &= \mathbf{0} \\ \rho(\mathbf{z}, \lambda) &= 0 \end{aligned} \tag{9}$$

The first vector equation in (9) corresponds to the steady-state system equations, which have a singular Jacobian $D_z\mathbf{F}|_0$ at the saddle-node bifurcation point $(\mathbf{z}_0, \lambda_0)$. The second scalar equation represents a phase condition $\rho : \Re^N \times \Re \mapsto \Re$ that guarantees non singularity of the corrector equations Jacobian

$$\left[ \begin{array}{cc} D_z\mathbf{F} & \dfrac{\partial \mathbf{F}}{\partial \lambda} \\ D_z\rho & \dfrac{\partial \rho}{\partial \lambda} \end{array} \right]_{(N+1)\times(N+1)}$$

at all equilibria on the bifurcation manifold.

Two different phase conditions $\rho(\cdot)$ have been successfully used in bifurcation studies of power systems. The first condition consists on defining a perpendicular vector to $\Delta\mathbf{z}_1$, which starts at $(\mathbf{z}_1 + \Delta\mathbf{z}_1, \lambda_1 + \Delta\lambda_1)$ and intersects the bifurcation manifold at $(\mathbf{z}, \lambda)$; thus,

$$\rho(\mathbf{z}, \lambda) = \Delta\mathbf{z}_1^T(\mathbf{z} - \mathbf{z}_1 - \Delta\mathbf{z}_1) + \Delta\lambda_1(\lambda - \lambda_1 - \Delta\lambda_1) \tag{10}$$

This was introduced in [22] and successfully applied to various systems in [6, 21]. This condition does not require of any kind of parameterization to guarantee non singularity of equations (9) for all system equilibria [16, 17].

A simpler phase condition was used in [23, 24, 25, 26], based on the local parameterization of the system around the bifurcation point. In this case, a local parameter $p$ ($\lambda$ or $z_i \in \mathbf{z}$), is set to a constant value, i.e.,

$$\rho(\mathbf{z}, \lambda) = p - p_1 - \Delta p_1$$

The parameter $p$ is chosen based on parameterization (5), guaranteeing a nonsingular Jacobian of equations (9) [20].

Of this two corrector techniques, the perpendicular intersection has the advantage of not requiring of parameterization. However, it introduces an almost full row in the Jacobian matrix, which must be taken into consideration during the factorization process to avoid sparsity degradation.

## 3. Fast-Decoupled Techniques

For certain ac system models, saddle-node bifurcations can be directly detected using load flow equations

$$\begin{aligned} \Delta\mathbf{P}(\delta, \mathbf{V}, \lambda) &= \mathbf{0} \\ \Delta\mathbf{Q}(\delta, \mathbf{V}, \lambda) &= \mathbf{0} \end{aligned} \tag{11}$$

since these equations have the same saddle-node transversality conditions as differential equations (2) [16, 17]. Hence, continuation methods can be applied to these equations to obtain the desired bifurcation diagram. $\Delta\mathbf{P}(\cdot)$ and $\Delta\mathbf{Q}(\cdot)$ are a subset of $\mathbf{F}(\cdot)$, and represent the active and reactive power mismatches at the system buses; the vectors $\mathbf{V}$ and $\delta$ stand for the bus phasor voltage magnitudes and angles, respectively.

Equations (11) can be efficiently solved for a given parameter value $\lambda^*$ using fast-decoupled load flow techniques [30, 31, 32]. Thus, during a Newton-Raphson iteration $i$ one has to solve matrix equation

$$\left[ \begin{array}{cc} D_\delta\Delta\mathbf{P}|_i & D_V\Delta\mathbf{P}|_i \\ D_\delta\Delta\mathbf{Q}|_i & D_V\Delta\mathbf{Q}|_i \end{array} \right] \left[ \begin{array}{c} \Delta\delta_i \\ \Delta\mathbf{V}_i \end{array} \right] = \left[ \begin{array}{cc} \mathbf{H}_i & \mathbf{N}_i \\ \mathbf{M}_i & \mathbf{L}_i \end{array} \right] \left[ \begin{array}{c} \Delta\delta_i \\ \Delta\mathbf{V}_i \end{array} \right] = \left[ \begin{array}{c} \Delta\mathbf{P}_{i-1} \\ \Delta\mathbf{Q}_{i-1} \end{array} \right] \tag{12}$$

for vector $[\Delta\delta_i^T \ \Delta\mathbf{V}_i^T]^T$, where $\Delta\mathbf{P}_{i-1} \triangleq \Delta\mathbf{P}(\delta_{i-1}, \mathbf{V}_{i-1}, \lambda^*)$, and $\Delta\mathbf{Q}_{i-1} \triangleq \Delta\mathbf{P}(\delta_{i-1}, \mathbf{V}_{i-1}, \lambda^*)$. Fast-decoupled methods are based first on the assumption that $\Delta\mathbf{V}_i \approx \mathbf{0}$ when solving (12), yielding equation

$$\mathbf{B}'\Delta\delta_i = \Delta\mathbf{P}(\delta_{i-1}, \mathbf{V}_{i-1}, \lambda^*) \tag{13}$$

Assuming then that $\Delta\mathbf{P}_i \approx \mathbf{0}$, leads to

$$\mathbf{B}''\Delta\mathbf{V}_i = \Delta\mathbf{Q}(\delta_{i-1} + \Delta\delta_i, \mathbf{V}_{i-1}, \lambda^*) \tag{14}$$

Equations (13) and (14) are solved sequentially (BX version). $\mathbf{B}'$ ($\mathbf{B}$ matrix) and $\mathbf{B}''$ ($\mathbf{X}^{-1}$ matrix) are constant matrices defined as [32]:

$$\begin{aligned} \mathbf{B}' &\triangleq \mathbf{H}|_{\delta=0, V=1} \\ \mathbf{B}'' &\triangleq \mathbf{L}|_{\delta=0, V=1, R=0} \end{aligned}$$

where $V\angle\delta$ stand for all bus phasor voltages, and $R$ represents all system resistances.

Similar assumptions can be used to solve the following corrector equations using the fast-decoupled method:

$$\begin{aligned} \Delta\mathbf{P}(\delta, \mathbf{V}, \lambda) &= \mathbf{0} \\ \Delta\mathbf{Q}(\delta, \mathbf{V}, \lambda) &= \mathbf{0} \\ \rho(\delta, \mathbf{V}, \lambda) &= 0 \end{aligned}$$

Thus, for the perpendicular intersection equation (10), the matrix equation of the $i^{th}$ Newton-Raphson iteration becomes

$$\left[ \begin{array}{ccc} \mathbf{H}_i & \mathbf{N}_i & \left.\dfrac{\partial\Delta\mathbf{P}}{\partial\lambda}\right|_i \\ \mathbf{M}_i & \mathbf{L}_i & \left.\dfrac{\partial\Delta\mathbf{Q}}{\partial\lambda}\right|_i \\ \Delta\delta_1^T & \Delta\mathbf{V}_1^T & \Delta\lambda_1 \end{array} \right] \left[ \begin{array}{c} \Delta\delta_i \\ \Delta\mathbf{V}_i \\ \Delta\lambda_i \end{array} \right] = \left[ \begin{array}{c} \Delta\mathbf{P}_{i-1} \\ \Delta\mathbf{Q}_{i-1} \\ \Delta\rho_{i-1} \end{array} \right]$$

where $\Delta\delta_1$, $\Delta\mathbf{V}_1$, and $\Delta\lambda_1$ are generated by the predictor step. Then, by assuming that $\Delta\delta_i \approx \mathbf{0}$, $\Delta\mathbf{V}_i \approx \mathbf{0}$, $\Delta\rho_i \approx 0$, and $\Delta\mathbf{P}_i \approx \mathbf{0}$, respectively, the following fast-decoupled corrector equations can be obtained:

$$\begin{aligned} \Delta\lambda_1\Delta\lambda_i &= \rho(\delta_{i-1}, \mathbf{V}_{i-1}, \lambda_{i-1}) \\ \mathbf{B}'\Delta\delta_i &= \Delta\mathbf{P}(\delta_{i-1}, \mathbf{V}_{i-1}, \lambda_{i-1} + \Delta\lambda_i) \\ \mathbf{B}''\Delta\mathbf{V}_i &= \Delta\mathbf{Q}(\delta_{i-1} + \Delta\delta_i, \mathbf{V}_{i-1}, \lambda_{i-1} + \Delta\lambda_i) \end{aligned} \tag{15}$$

These equations can be solved sequentially to obtain the desired equilibrium point on the bifurcation manifold. For small

changes $\Delta\delta_1$ and $\Delta\mathbf{V}_1$, i.e., small variations in the system variables $\mathbf{z}$, equations (15) can be shown to have similar convergence characteristics as fast-decoupled load flow equations (13) and (14). The latter condition can be met by reducing the predictor's parameter step $\Delta\lambda_1$ as the system approaches a saddle-node bifurcation.

HVDC systems can be included in these fast-decoupled techniques by treating the ac/dc converters at each iteration as constant PQ loads, while updating the system ac bus voltages, and then solving the DC system equations with fixed ac converter voltages to calculate new values of the corresponding ac active and reactive powers; this process is repeated until achieving convergence.

Although the proposed fast-decoupled corrector has not been implemented and tested, the previous analysis justifies incorporating this technique into an existing continuation power flow program. Work is currently underway at the University of Waterloo to add these methods to the PFLOW program originally developed at the University of Wisconsin-Madison [6].

A secant predictor together with the fast-decoupled corrector described above were proposed for inclusion in future versions of EPRI's program VSTAB [27]. The current version of this program does not have a true implementation of a predictor-corrector continuation algorithm; however, the program successfully uses fast-decoupled load flows to determine s.e.p.s on the bifurcation manifold for fixed values of $\lambda$, which could be viewed as a fast-decoupled implementation of the fixed parameter corrector described above, without local parameterizations. When the fast-decoupled method fails to converge, the program switches to a full Newton-Raphson iteration.

## 4. System Reduction

Another approach to reduce the computational burden of tracing bifurcation diagrams and locating bifurcation points, is to reduce the system size while maintaining acceptable levels of accuracy in the calculations. A method to reduce the number of system variables for these types of studies was proposed in [28]; in this case, the system is reduced based on coherency considerations. This paper proposes two different methods to reduce the system size, based on certain local characteristics of saddle-node bifurcations. A discussion of these techniques follows.

### *4.1. Tangent Vector Technique*

Saddle-node bifurcations in power systems can be associated to angle and/or voltage magnitude problems at specific system buses through the zero right-eigenvector [6, 12, 16, 29]. This can be easily justified based on the fact that the tangent vector $d\mathbf{z}/d\lambda$ converges to this eigenvector at the bifurcation point [16, 17]; hence, the largest entries on the zero right-eigenvector pinpoint the critical areas and buses affected the most by the bifurcation. On the other hand, small entries on this vector indicate that the bifurcation has little steady-state effect on the corresponding system variables or buses. Based on this observations, the system variables that suffer little changes during the calculation of the bifurcation diagram, can be safely eliminated from the computational process without affecting the final results, i.e., a variable $z_i \in \mathbf{z}$ can be kept constant at its last equilibrium value if

$$|\Delta z_{i_1}| \leq u$$

where $\Delta z_{i_1} \in \Delta\mathbf{z}_1$ in (4), and $u$ is a user defined tolerance. Notice that vector $\Delta\mathbf{z}_1$ has been already normalized, which avoids errors of elimination of important system variables due to small values of all entries in $d\mathbf{z}/d\lambda|_1$, especially for "flat" bifurcation profiles far from the bifurcation. This technique reduces the number of variables and equations used during the continuation process, decreasing consequently the computational burden of tracing bifurcation diagrams.

A problem with this method is the possible elimination of variables associated to system controls with limits, particularly bus voltages with large reactive power support. These voltages change slowly or do not change at all, until voltage control is lost when minimum or maximum limits are reached. Furthermore, depending on the system variations produced by the parameter $\lambda$, an area that initially is not considered critical due to small changes on the associated system variables, could become critical when close to bifurcation. Hence, variables that are eliminated in early stages of the continuation process, might become later a source for significant computational errors. To minimize this problem one can allow for the inclusion of these variables as they start changing rapidly; however, this procedure implies having to calculate the tangent vector for the full system every few steps, eliminating some of the computational benefits of the proposed reduction technique. A simpler but effective approach is to carry out a system reduction every $U$ steps of the continuation method.

This reduction technique was implemented into the PFLOW program [6], and tested in the 300 bus IEEE system. The results of these tests and some additional computational issues are presented and discussed in section 5.

### *4.2. Network Partition*

Several network partition techniques have been proposed to reduce the size of the power system for steady-state voltage stability analysis [33, 34, 35]. These methods also yield the critical areas and buses in the system, so that control actions can be taken to steer the system away from the bifurcation point. A new method based on these techniques is proposed here to partition the system and reduce the computational burden of calculating the bifurcation manifold.

The idea is to first detect the critical bus for a given operating point, i.e., determine the load bus with the largest voltage variations when the system parameter $\lambda$ is changed. This can be easily done using the tangent vector generated by the predictor step. The largest entry on that vector determines the critical system variable and its associated load bus, as discussed above. Once the critical bus is located, an initial critical area is formed with the first neighbors of this bus (level 1). New levels of neighboring buses can be added to this basic critical area to increase its size. The buses that do not belong to the critical area but connect this area to the rest of the system (border buses), are considered as part of the reduced system and are treated as constant voltage buses, i.e., PV buses, based on the assumption that their steady-state voltage magnitudes are not significantly affected by the parameter changes in the system. Hence, to determine a connection level that defines an adequate system partition, one of the following criteria can be used:

- Determine the determinant of the "critical matrix" $\mathbf{D}'$ for the full and partitioned systems, as defined in [34], i.e.,

$$\begin{aligned} \mathbf{D}' &\triangleq \mathbf{D} - \mathbf{C}\mathbf{A}^{-1}\mathbf{B} \qquad (16) \\ \Rightarrow \quad \det\left(D_z\mathbf{F}|_1\right) &= \det\left(\mathbf{D}'\right)\det\left(\mathbf{A}\right) \end{aligned}$$

where matrices $\mathbf{A}$, $\mathbf{B}$, $\mathbf{C}$ and $\mathbf{D}$ are part of the system Jacobian matrix $D_z\mathbf{F}|_1$ evaluated at the equilibrium point $(\mathbf{z}_1, \lambda_1)$,

$$D_z\mathbf{F}|_1 = \begin{bmatrix} \mathbf{A} & \mathbf{B} \\ \mathbf{C} & \mathbf{D} \end{bmatrix}$$

$\mathbf{D}$ is a $2 \times 2$ matrix partition corresponding to equations and variables of the critical bus $l$, thus

$$\mathbf{D} \triangleq \begin{bmatrix} \left.\frac{\partial \Delta P_l}{\partial \delta_l}\right|_1 & \left.\frac{\partial \Delta P_l}{\partial V_l}\right|_1 \\ \left.\frac{\partial \Delta Q_l}{\partial \delta_l}\right|_1 & \left.\frac{\partial \Delta Q_l}{\partial V_l}\right|_1 \end{bmatrix}$$

where $[\Delta P_l(\cdot)\ \Delta Q_l(\cdot)]^T \in \mathbf{F}(\cdot)$, and $[\delta_l\ V_l]^T \in \mathbf{z}$. Notice that $\mathbf{D}'$ for the complete and reduced systems in (16), can be obtained by factorizing the corresponding Jacobian matrix $D_z\mathbf{F}|_1$. Furthermore, since $D_z\mathbf{F}|_1$ is nonsingular for all equilibrium points other than the saddle-node bifurcation $(\mathbf{z}_0, \lambda_0)$, $\det(\mathbf{D}') \neq 0$ and $\det(\mathbf{A}) \neq 0$ for those equilibria. (At the bifurcation point $\det(\mathbf{D}') = 0$ and $\det(\mathbf{A}) \neq 0$, since $\det(D_z\mathbf{F}|_0) = 0$ and matrix $\mathbf{A}$ is nonsingular, due to the elimination from the singular Jacobian $D_z\mathbf{F}|_0$ of the rows and columns with the largest entries in the zero right-eigenvector.) Hence, by monitoring the difference between the determinants of $\mathbf{D}'_F$ for the full system and $\mathbf{D}'_R$ for the reduced system, an adequate partition is assumed to be obtained when

$$\Big|\ |\det(\mathbf{D}'_R)| - |\det(\mathbf{D}'_F)|\ \Big| \leq \epsilon \qquad (17)$$

where $\epsilon$ is a positive scalar that defines the desired criterion tolerance.

- Compare the changes in the tangent vector $\mathrm{d}\mathbf{z}/\mathrm{d}\lambda|_1$ between the full and the reduced system. Thus, when

$$\left|\ \|\left.\frac{\mathrm{d}\mathbf{z}_R}{\mathrm{d}\lambda}\right|_1\| - \|\left.\frac{\mathrm{d}\mathbf{z}_F}{\mathrm{d}\lambda}\right|_1\|\right| \leq \epsilon \qquad (18)$$

the desired system reduction level is attained. When the tangent vector predictor is used, the computational cost of applying this criterion is lower than calculating matrices $\mathbf{D}'$, since one only needs to solve equation (3) for each reduction level until convergence condition (18) is met.

Of these two criteria, the tangent vector appears to be more sensible to changes in system size than the determinant of $\mathbf{D}'$; however, the norm of $\mathrm{d}\mathbf{z}/\mathrm{d}\lambda$ seems to have a highly nonlinear behavior with respect to changes in $\lambda$, similar to the previously depicted behavior of the Jacobian eigenvalues, whereas the determinant of the reduced matrix associated to the critical bus seems to have an almost linear behavior as shown in [36]. More tests have to be carried out before a definite conclusion can be reached.

This reduction process can be repeated every few steps of the continuation method, and as with the tangent vector reduction method, one expects to obtain a smaller critical area partition as the system approaches bifurcation.

Since the parameter $\lambda$ is usually chosen to simulate varying load levels throughout the system, the corresponding generator powers must also be allowed to change to supply the desired system load for each value of $\lambda$. For the full system this does not represent a problem; all system generators are assigned a participation factor of the total available power, depending on its size and initial active and reactive powers, so that each generator can change its base power to supply the desired load demand. For the reduced system, where some, or all, border buses have been converted from load (PQ) to generator (PV) buses, one must first determine the level of power that is being delivered to or absorbed from the critical area through these buses, so that an appropriate generation participation factor can be defined. Hence, these factors can be calculated by comparing the power change on these buses for two different equilibria on the bifurcation manifold, i.e., for two distinct values of $\lambda$ the power differences on the border buses yield the desired participation factors.

One problem that still has to be resolved in order to make the proposed method a practical tool, is the handling of voltage control limits, particularly generator Q-limits, which make a significant difference in the shape of the bifurcation manifolds and the location of the corresponding bifurcation points, as illustrated in section 5 and discussed in [4, 6, 21]. Studies are underway to find an appropriate answer to this question, but so far it does not appear to have a simple solution.

The partition technique presents the same problem as the tangent vector reduction method regarding the possible changes in location of the critical area with changes on the parameter $\lambda$. Hence, if the critical area at the bifurcation is not part of the reduced system, the final results can have significant errors as demonstrated for the 300 bus IEEE test system below. This is especially true for the partition method, which, contrary to the tangent vector technique, is based on a local area analysis of the system; therefore, this method seems to be better suited to handle problems where changes in $\lambda$ only affect a particular area in the system.

Due to the unresolved difficulties in the partition method, it was not directly implemented in an existing continuation program. The preliminary results shown in the next section were obtained using the PFLOW program [6] and MATLAB [37].

## 5. Computational Results

The 300 bus IEEE system was used to test the system reduction techniques described above. This is an ac system divided in 3 areas, with 69 generators and 411 transmission lines and transformers, including 51 under-load tap changer (ULTC) transformers. The tests were carried without enforcing power flow control between areas and treating the ULTCs as regular transformers with fixed taps, to simplify the analysis of the results. The system loads were modeled as constant PQ loads, and the parameter $\lambda$ was used to simulate active and reactive power load increases throughout the system, i.e., load powers at bus $j$ were simulated as

$$\begin{aligned} P_j &= P_j^0(1+\lambda) \\ Q_j &= Q_j^0(1+\lambda) \end{aligned}$$

where $P_j^0$ and $Q_j^0$ represent the base load power. For this particular load model, $\lambda$ represents the loading factor in p.u. or total MVA. The generators were assigned a participation fac-

tor of the load demand based on the initial generated power, without enforcing maximum active power limits. Several tests were run with and without generator Q-limits, as shown below.

The tangent vector reduction technique was incorporated into the PFLOW program, to obtain the results shown in Tables 1 through 4 for several values of the tolerance $u$ and number of steps $U$ in (18). Figures 3–6 depict the bifurcation diagrams corresponding to each of the test cases in Tables 1–4; the tip of these curves correspond to a saddle-node bifurcation. No distinction is made between stable (s.e.p.) and unstable (u.e.p.) equilibrium points on these manifolds, since the eigenvalues were only monitored to detect a singularity or saddle-node bifurcation point; Hopf bifurcations were not tracked on these cases.

Tables 2 and 1, and their corresponding Figs. 4 and 3, show the results obtained for increasing load throughout the whole system, with and without enforcing generator Q-limits, respectively. On the other hand, Tables 4 and 3 with their respective Figs. 6 and 5, depict the results obtained with and without Q-limits when the load is changed in area 3 only. From these results one can conclude, in general, that the smaller the values of $u$ and $U$, the smaller the number of equations and, therefore, the larger the errors. Also, as the criterion tolerance $u$ and the number of steps $U$ decreases, the CPU time per step of the continuation method tends to decrease, as expected, particularly for the cases where the load is only changing in a small system area. Notice that in some cases the CPU time tends to increase even though the number of equations decreases, this is due to the need of having to refactorize the Jacobian matrix when the equations change; thus, the smaller the value of $U$, the more often this has to be done along the bifurcation manifold, and consequently the larger the CPU time. In some cases cycling and back-tracking problems were detected, especially when the values of $u$ and $U$ are small, increasing the overall CPU time required to trace the bifurcation manifolds.

Figure 6 depicts the problem of immediate Q-limit instability [4, 5, 6], i.e., the test system becomes immediately unstable when voltage control is lost at generator bus 191.

Table 5 and Fig. 7 depict the results and bifurcation manifold, respectively, obtained with the network partition method when using convergence criterion (17) with $\epsilon = 10^{-4}$. The load powers are assumed to increase in all system load buses without generator Q-limit enforcement. The saddle-node bifurcation $\lambda_{max}$ values and critical buses shown in Table 5 were obtained using a direct method. CPU times were not determined in this case since the method was not incorporated into a continuation program; the test shown here was run only to depict some of the problems with the partition method. Notice that by using the determinant convergence criterion the system is reduced from 300 buses to 110 (level 9) at the initial operating point, i.e., for $\lambda = 0$. This reduced system does not contain the critical bus at the saddle-node bifurcation point (bus 191), consequently yielding a significant error in the bifurcation manifold depicted in Fig. 5, and in the location of the corresponding bifurcation point. More tests must be run to determine whether tangent vector criterion (18) yields better results, and to resolve the problem of how to handle voltage control limits.

| Case No. | Reduction Data | Eqns. | Time [sec.] | Time/step [sec.] | $\lambda_{max}$ [p.u.] | $\lambda$ Error [%] |
|---|---|---|---|---|---|---|
| 1 | $u = 0$ $U = \infty$ | 600 | 43.2 | 1.4897 | 0.36908 | -0.07 |
| 2 | $u = 10^{-6}$ $U = 2$ | 596 | 46.7 | 1.6103 | 0.36908 | -0.07 |
| 3 | $u = 10^{-4}$ $U = 2$ | 460 | 46.2 | 1.5931 | 0.36908 | -0.07 |
| 4 | $u = 10^{-3}$ $U = 10$ | 407 | 46.5 | 1.6034 | 0.37337 | +1.09 |
| 5 | $u = 10^{-3}$ $U = 5$ | 395 | 51.6 | 1.7793 | 0.37598 | +1.80 |
| 6† | $u = 10^{-3}$ $U = 2$ | 64 | 67.1 | 1.7205 | 0.37968 | +2.80 |

†Cycling problems in the u.e.p. region

**Table 1:** *Results of the tangent vector reduction technique for the 300 bus IEEE system with* no limits *considered, when the active and reactive load powers are increased throughout the system. The direct method applied to the complete system yields:* $\lambda_{max} = 0.36934 p.u.$*, and bus 191 as the critical bus.*

| Case No. | Reduction Data | Eqns. | Time [sec.] | Time/step [sec.] | $\lambda_{max}$ [p.u.] | $\lambda$ Error [%] |
|---|---|---|---|---|---|---|
| 7 | $u = 0$ $U = \infty$ | 600 | 75.6 | 1.3263 | 0.04575 | -0.03 |
| 8 | $u = 10^{-6}$ $U = 2$ | 598 | 76.9 | 1.3491 | 0.04575 | -0.03 |
| 9 | $u = 10^{-4}$ $U = 2$ | 582 | 82.0 | 1.4386 | 0.04563 | -0.29 |
| 10 | $u = 10^{-3}$ $U = 10$ | 513 | 87.1 | 0.9678 | 0.04927 | +7.67 |
| 11† | $u = 10^{-3}$ $U = 5$ | 446 | 114.6 | 1.6141 | 0.04943 | +8.01 |
| 12† | $u = 10^{-3}$ $U = 2$ | 450 | 104.4 | 1.5353 | 0.04953 | +8.23 |

†Back-tracking

**Table 2:** *Results of the tangent vector reduction technique for the 300 bus IEEE system with* limits *considered, when the active and reactive load powers are increased throughout the system. The direct method applied to the complete system yields:* $\lambda_{max} = 0.04576 p.u.$*, and bus 576 as the critical bus.*

| Case No. | Reduction Data | Eqns. | Time [sec.] | Time/step [sec.] | $\lambda_{max}$ [p.u.] | $\lambda$ Error [%] |
|---|---|---|---|---|---|---|
| 13 | $u = 0$ $U = \infty$ | 600 | 48.9 | 1.4382 | 1.0002 | -0.08 |
| 14 | $u = 10^{-6}$ $U = 2$ | 451 | 76.2 | 2.2412 | 1.0082 | +0.71 |
| 15† | $u = 10^{-4}$ $U = 2$ | 263 | 47.7 | 1.1634 | 1.0466 | +4.55 |
| 16 | $u = 10^{-3}$ $U = 10$ | 161 | 49.3 | 1.1465 | 1.3928 | +39.13 |
| 17 | $u = 10^{-3}$ $U = 5$ | 163 | 36.0 | 1.0000 | 1.1085 | +10.73 |
| 18† | $u = 10^{-3}$ $U = 2$ | 136 | 54.8 | 0.8839 | 1.9209 | +91.89 |

†Back-tracking

**Table 3:** *Results of the tangent vector reduction technique for the 300 bus IEEE system with* no limits *considered, when the active and reactive load powers are increased in a particular area of the system only. The direct method applied to the complete system yields:* $\lambda_{max} = 1.00105 p.u.$*, and bus 191 as the critical bus.*

| Case No. | Reduction Data | Eqns. | Time [sec.] | Time/step [sec.] | $\lambda_{max}$ [p.u.] | $\lambda$ Error [%] |
|---|---|---|---|---|---|---|
| 19 | $u = 0$ $U = \infty$ | 600 | 77.8 | 1.2754 | 0.12021 | 0 |
| 20 | $u = 10^{-6}$ $U = 2$ | 535 | 81.0 | 1.5577 | 0.12021 | 0 |
| 21 | $u = 10^{-4}$ $U = 2$ | 324 | 46.5 | 1.2237 | 0.12050 | +0.24 |
| 22 | $u = 10^{-3}$ $U = 10$ | 211 | 43.2 | 1.1077 | 0.12110 | +0.74 |
| 23 | $u = 10^{-3}$ $U = 5$ | 210 | 41.5 | 1.0921 | 0.12192 | +1.42 |
| 24 | $u = 10^{-3}$ $U = 2$ | 210 | 40.0 | 1.1111 | 0.12231 | +1.75 |

**Table 4:** *Results of the tangent vector reduction technique for the 300 bus IEEE system with* limits *considered, when the active and reactive load powers are increased in a particular area of the system only. The system becomes immediately unstable before the saddle-node bifurcation when a maximum Q-limit is reached at bus 191 when* $\lambda_{Q_{lim}} = 0.12021 p.u.$

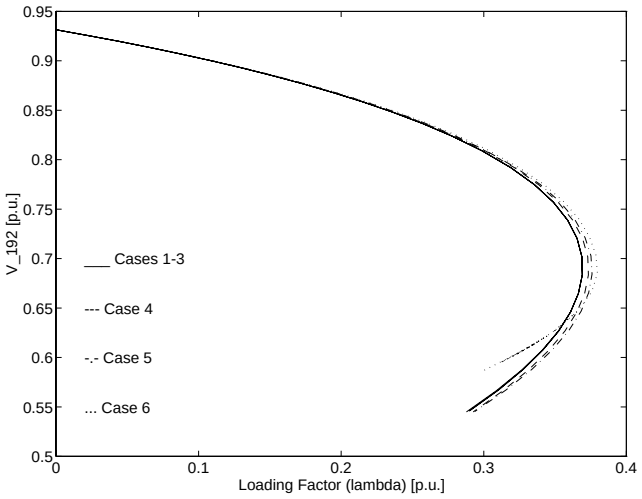


**Fig. 3:** *Bifurcation diagrams (PV or nose curves) of a system bus voltage for the original and reduced systems when* no limits *are considered. The active and reactive powers increase in all system load buses. A saddle-node bifurcation takes place at the maximum system loading* $\lambda_{max} = 0.36934 p.u.$

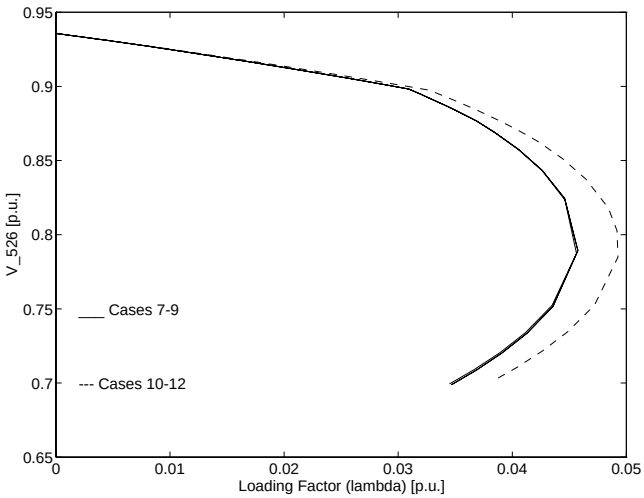


**Fig. 4:** *Bifurcation diagrams (PV or nose curves) of a system bus voltage for the original and reduced systems when* limits *are considered. The active and reactive powers increase in all system load buses. A saddle-node bifurcation takes place at the maximum system loading* $\lambda_{max} = 0.04576 p.u.$

| Case No. | Buses | Gens. | Critical Bus | $\det(D')$ | $\lambda_{max}$ [p.u.] | $\lambda$ Error [%] |
|---|---|---|---|---|---|---|
| 1 | 300 | 69 | 191 | 0.0211 | 0.36934 | 0 |
| 25 | 110 | 36 | 9025 | 0.0210 | 0.59566 | +61.28 |

**Table 5:** *Results of the network partition reduction technique for the 300 bus IEEE system with no generator Q-limits and load increasing throughout the system.*

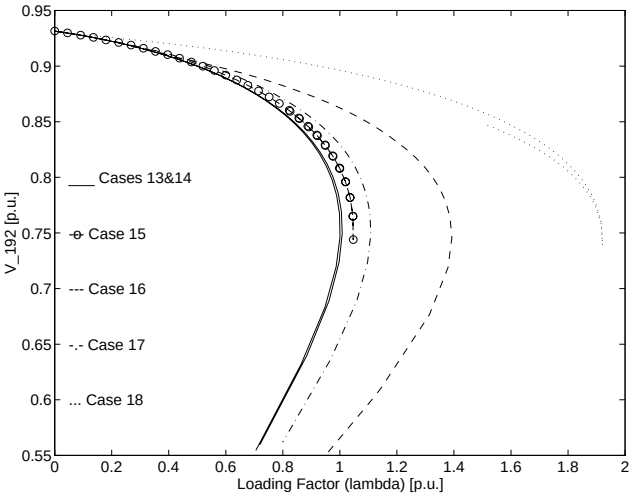


**Fig. 5:** *Bifurcation diagrams (PV or nose curves) of a system bus voltage for the original and reduced systems when* no limits *are considered. The active and reactive load powers increase in a local area only. A saddle-node bifurcation takes place at the maximum system loading* $\lambda_{max} = 1.00105 p.u.$

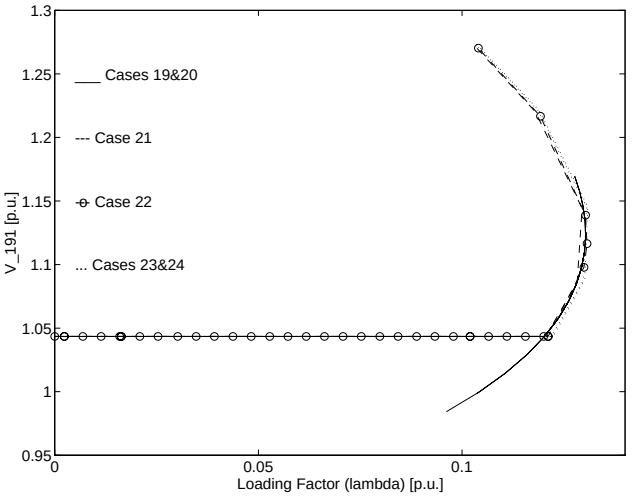


**Fig. 6:** *Bifurcation diagrams (PV or nose curves) of a system bus voltage for the original and reduced systems when* limits *are considered. The active and reactive load powers increase in a local area only. A Q-limit immediate instability occurs at* $\lambda_{Q_{lim}} = 0.12021 p.u.$*, before the saddle-node bifurcation point.*

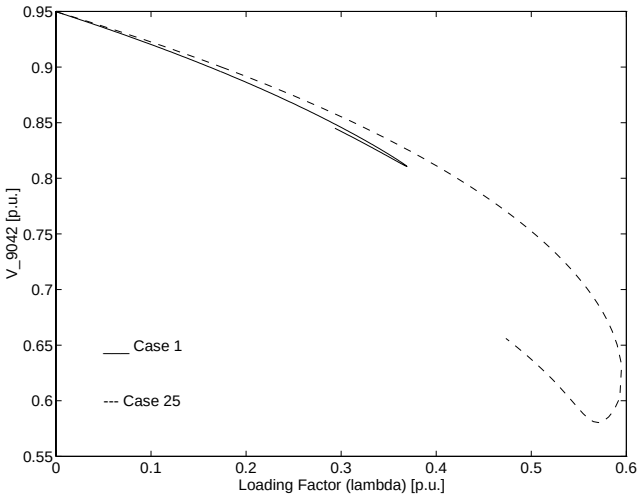


**Fig. 7:** *Bifurcation diagrams (PV or nose curves) of a system bus voltage for the original and partitioned systems when no limits are considered and the active and reactive load powers increase throughout the system. A saddle-node bifurcation takes place at the maximum system loading* $\lambda_{max} = 0.36934 p.u.$

## 6. Conclusions

A comprehensive review of the current literature and state of the art of continuation methods in power systems bifurcation analysis is presented. The paper then proposes three different methods to accelerate the computation of saddle-node bifurcation points and their associated manifolds with the continuation method, namely, fast-decoupled correctors, tangent vector system reduction, and network partition. Of these methods, only the tangent vector was incorporated and tested in a the production-grade continuation program PFLOW; however, additional tests on larger systems are required.

Work is currently underway to include and test the proposed fast-decoupled corrector in PFLOW, based on favorable previous experience with successive fast-decoupled power flows in VSTAB. In the case of system reduction through network partition, several issues, particularly the handling of voltage control limits, have to be resolved before this method can be programmed and tested in realistic conditions. Once all these methods are implemented in a similar computational environment, a thorough comparison of their performance will be carried out to determine their applicability in control centers.

## REFERENCES


[1] L. H. Fink, ed., *Proceedings: Bulk Power System Voltage Phenomena—Voltage Stability and Security*, ECC/NSF Workshop, Fairfax, VA, Ecc. Inc., August 1991.

[2] Y. Mansour, ed., *Suggested Techniques for Voltage Stability Analysis*, IEEE/PES Report, 93TH0620-5PWR, 1993.

[3] C. C. Liu and K. T. Vu, "Types of Voltage Collapse," in [1], pp. 133–141.

[4] I. Dobson and L. Lu, "Voltage Collapse Precipitated by the Immediate Change in Stability When Generator Reactive Power Limits are Encountered," *IEEE Trans. Circuits and Syst.-I*, Vol. 39, No. 9, September 1992, pp. 762–766.

[5] G. K. Morrison, B. Gao, P. Kundur, "Voltage Stability Analysis Using Static and Dynamic Approaches," *IEEE Trans. Power Systems*, Vol. 8, No. 3, August 1993, pp. 1159–1171.

[6] C. A. Cañizares and F. L. Alvarado, "Point of Collapse and Continuation Methods for Large AC/DC Systems," *IEEE Trans. Power Systems*, Vol. 8, No. 1, February 1993, pp. 1–8.

[7] M. M. Begovic and A. G. Phadke, "Dynamic Simulation of Voltage Collapse," *IEEE Trans. Power Systems*, Vol. 5, No. 4, November 1990, pp. 1529–1534.

[8] H. G. Kwatny, A. K. Pasrija, L. Y. Bahar, "Static Bifurcations in Electric Power Networks: Loss of Steady-State Stability and Voltage Collapse," *IEEE Trans. Circuits and Syst.*, Vol. 33, No. 10, October 1986, pp. 981–991.

[9] I. Dobson and H. D. Chiang, "Towards a Theory of Voltage Collapse in Electric Power Systems," *Systems & Control Letters*, Vol. 13, 1989, pp. 253–262.

[10] C. A. Cañizares, "On Bifurcations, Voltage Collapse and Load Modeling," *IEEE/PES 94 SM 512-4-PWRS*, San Francisso, July 1994.

[11] C. A. Cañizares, F. L. Alvarado, C. L. DeMarco, I. Dobson, W. F. Long, "Point of Collapse Methods Applied to AC/DC Power Systems," *IEEE Trans. Power Systems*, Vol. 7, No. 2, May 1992, pp. 673–683.

[12] B. Gao, G. K. Morrison, P. Kundur, "Voltage Stability Evaluation Using Modal Analysis," *IEEE Trans. Power Systems*, Vol. 7, No. 4, November 1992, pp. 1529–1542.

[13] P. A. Löf, T. Smed, G. Anderson, D.J. Hill, "Fast Calculation of a Voltage Stability Index," *IEEE Trans. Power Systems*, Vol. 7, No. 1, February 1992, pp. 54–64.

[14] J. Deuse and M. Stubbe, "Dynamic Simulation of Voltage Collapses," *IEEE Trans. Power Systems*, Vol. 8, No. 3, August 1993, pp. 894–904.

[15] V. Ajjarapu and B. Lee, "Bifurcation Theory and its Application to Nonlinear Dynamical Phenomena in an Electrical Power System," *IEEE Trans. Power Systems*, Vol. 7, No. 2, February 1992, pp. 424–431.

[16] C. A. Cañizares, "Conditions for saddle-node bifurcations in AC/DC power Systems," accepted for publication in the *Int. J. of Electric Power & Energy Systems*, May 1994.

[17] C. A. Cañizares, "Saddle-Node Bifurcations in Power Systems," *Proc. JIEE*, Quito, Ecuador, July 1993, pp. 222–229.

[18] C. A. Cañizares and S. Hranilovic, "Transcritical and Hopf Bifurcations in AC/DC Systems," *Proc. Bulk Power System Voltage Phenomena–III Seminar*, NSF/ECC Inc., Davos, Switzerland, August 1994.

[19] J. Guckenheimer and P. Holmes, *Nonlinear Oscillations, Dynamical Systems, and Bifurcations of Vector Fields*, Springer-Verlag, New York, 1986.

[20] R. Seydel, *From Equilibrium to Chaos—Practical Bifurcation and Stability Analysis*, Elsevier Science Publishers, North-Holland, 1988.

[21] C. A. Cañizares, W. F. Long, F. L. Alvarado, C. L. DeMarco, "Techniques for Detecting Proximity to Voltage Collapse in AC/DC Systems," *Proc. III SEPOPE*, Belo Horizonte, Brazil, May 1992, paper IP-18.

[22] K. Iba, H. Suzuki, M. Egawa, T. Watanabe, "Calculation of Critical Loading Condition with Nose Curve Using Homotopy Continuation Method," *IEEE Trans. Power Systems*, Vol. 6, No. 2, May 1991, pp 584–593.

[23] V. Ajjarapu and C Christy, "The Continuation Power Flow: A Tool for Steady State Voltage Stability Analysis," *IEEE Trans. Power Systems*, Vol. 7, No. 1, February 1992, pp. 416–423.

[24] V. Ajjarapu, N. Jain, Z. Yu, S. Battula, "Recent Developments to the Continuation Power Flow," *Proc. NAPS*, Washington, October 1993, pp. 205–214.

[25] H. D. Chiang, W. Ma, R. J. Thomas, J. S. Thorp, "A Tool for Analyzing Voltage Collapse in Electric Power Systems," *Proc. PSCC*, Graz, Austria, August 1990, pp. 1210–1217.

[26] H. D. Chiang, A. J. Flueck, K. S. Shah, N. Balu, "CPFLOW: A Practical Tool for Tracing Power System Steady-State Stationary Behavior Due to Load and Generation Variations," *IEEE/PES 94 WM 244-4-PWRD*, New York, February 1994.

[27] *Voltage Stability/Security Assessment and On-Line Control*, EPRI TR-101931, Vol. 1, April 1993.

[28] M. M. Begovic and A. G. Phadke, "Voltage Stability Assessment Through Measurement of a Reduced State Vector," *IEEE Trans. Power Systems*, Vol. 5, No. 1, February 1990, pp. 198–203.

[29] I. Dobson, "Observations on the Geometry of Saddle Node Bifurcations and Voltage Collapse in Electrical Power Systems," *IEEE Trans. Circuits and Syst.–I*, Vol. 39, No. 3, March 1992, pp. 240–243.

[30] B. Stott and O. Alsaç, "Fast Decoupled Load Flow," *IEEE Trans. Power Apparatus and Systems*, Vol. 93, 1974, pp. 859–869.

[31] R. A. M. van Amerongen, "A General-Purpose Version of the Fast Decoupled Load Flow," *IEEE Trans. Power Systems*, Vol. 4, No. 2, May 1989, pp. 760–770.

[32] A. Monticelli, A. Garcia, O. R. Saavedra, "Fast Decoupled Load Flow: Hypothesis, Derivations, and Testing," *IEEE Trans. Power Systems*, Vol. 5, No. 4, November 1990, pp. 1425–1431.

[33] L. Vargas and V. H. Quintana, "Clustering Techniques for Voltage Collapse Detection," *Electric Power System Research*, Vol. 23, No. 1, 1993, pp. 53–59.

[34] A. C. Z. de Souza and V. H. Quintana, "Identification of Voltage Collapse Using Network Partitioning," *Proc. NAPS*, Washington, October 1993, pp. 191–196.

[35] A. C. Z. de Souza and V. H. Quintana, "A New Technique of Network Partitioning for Voltage Collapse Margin Calculations," paper GTD/93/2181 accepted for publication on *IEE Proc. Generation, Transmission and Distribution*, June 1994.

[36] A. C. Z. de Souza, "A Voltage Collapse Approach by Critical Bus Determination," *Ph.D. Research Proposal*, E&CE Department, University of Waterloo, April 1994.

[37] *MATLAB*, The Math Works Inc., Natick, Massachusetts, 1993.

**Claudio A. Cañizares** was born in Mexico, D.F. in 1960. In April 1984, he received the Electrical Engineer diploma from the Escuela Politécnica Nacional (EPN), Quito-Ecuador, where he was a professor for several years. His MS (1988) and PhD (1991) degrees in Electrical Engineering are from the University of Wisconsin–Madison. Dr. Cañizares is currently an Assistant Professor at the University of Waterloo, Department of Electrical & Computer Engineering, and his research activities are mostly concentrated in the analysis of stability issues in ac/dc systems.

**Antonio Z. de Souza** was born in Brazil, on December 15, 1963. He received his B.Sc. in Electrical Engineering from the University of the State of Rio de Janeiro in 1987. In September 1990, he obtained his M.Sc. degree in Electrical Engineering at the Catholic Pontifical University of Rio de Janeiro. He has been working towards a Ph.D. degree at University of Waterloo, Department of Electrical and Computer Engineering, since September 1992, sponsored by the Brazilian agency CNPq. His research interests are in restoration and voltage control of power systems.

**Victor H. Quintana** received the Dipl. Ing. degree from the State Technical University of Chile in 1959, and the M.Sc. and Ph.D. degrees in Electrical Engineering from the University of Wisconsin, Madison in 1965, and University of Toronto, Ontario, in 1970, respectively. Since 1973 he has been with the University of Waterloo, Department of Electrical and Computer Engineering, where he is currently a Full Professor and Associate Chairman for Graduate Studies. His main research interests are in the areas of numerical optimization techniques, state estimation and control theory as applied to power systems.

Dr. Quintana is an Associate Editor of the International Journal of Energy Systems, and a member of the Association of Professional Engineers of the Province of Ontario.